Modeling The Effects of Longwall Mining on the Ground Water System
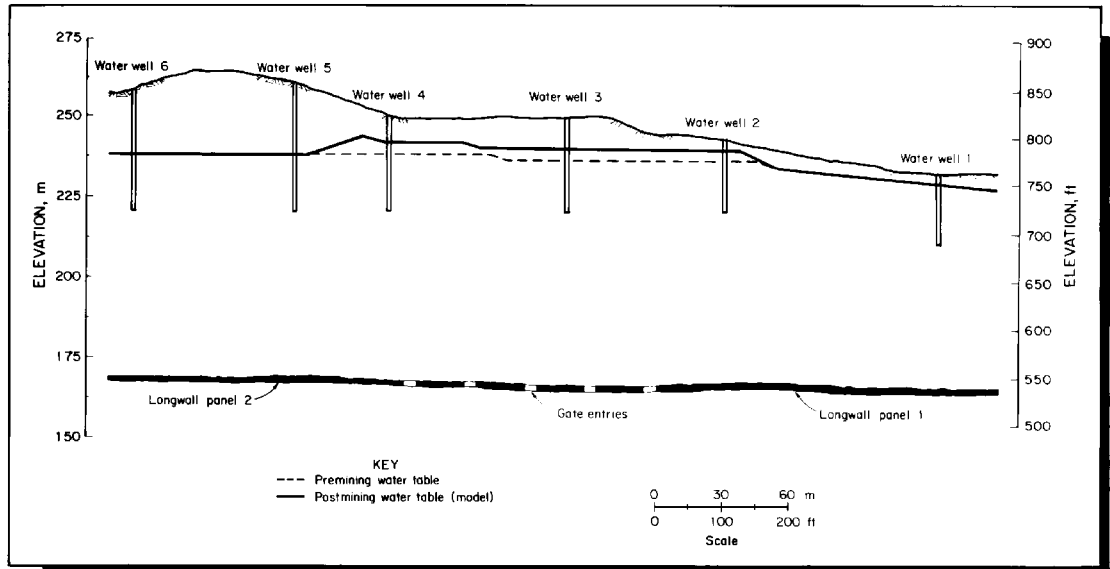
By R. J. Matetic, J. Liu, and D. Elsworth

U.S. Department of the Interior
Mission Statement

As the Nation's principal conservation agency, the Department of the Interior has responsibility for most of our nationally-owned public lands and natural resources. This includes fostering sound use of our land and water resources; protecting our fish, wildlife, and biological diversity; preserving the environmental and cultural values of our national parks and historical places; and providing for the enjoyment of life through outdoor recreation. The Department assesses our energy and mineral resources and works to ensure that their development is in the best interests of all our people by encouraging stewardship and citizen participation in their care. The Department also has a major responsibility for American Indian reservation communities and for people who live in island territories under U.S. administration.

Cover: Predicted postmining effects to the groundwater system utilizing finite-element model.

Report of Investigations 9561

Modeling The Effects of Longwall Mining on the Ground Water System

By   R. J. Matetic, J. Liu, and D. Elsworth

CONTENTS

ILLUSTRATIONS

TABLES

UNIT OF MEASURE ABBREVIATIONS USED IN THIS REPORT

<u>Metric Units</u>

cm	centimeter	m/s^2	meter per square second
kg/m^3	kilogram per cubic meter	m/yr	meter per year
Lpm	liter per minute	m^2/s	square meter per second
m	meter	mm	millimeter
m/km	meter per kilometer	MPa	mega pascal
m/s	meter per second		

<u>U.S. Customary Units</u>

ft	foot	gpm	gallon per minute
ft/mi	foot per mile	h	hour
ft/s	foot per second	in	inch
ft/s^2	foot per square second	lb/ft^2	pound per square foot
ft/yr	foot per year	lb/ft^3	pound per cubic foot
ft^2/s	square foot per second	psi	pound (force) per square inch

MODELING THE EFFECTS OF LONGWALL MINING ON THE GROUND WATER SYSTEM

By R. J. Matetic,[1] J. Liu,[2] and D. Elsworth[3]

ABSTRACT

The objective of this U.S. Bureau of Mines hydrologic-subsidence investigation was to evaluate the effects of longwall mining on the local ground water regime through field monitoring and numerical modeling. Field data were obtained from multiple-position borehole extensometers (MPBX's) that were used to measure subsurface displacements. Survey monuments were installed to measure mining-induced surface deformations. Numerous drawdown and recovery tests were performed to characterize hydrologic properties of the overburden strata. Coreholes were drilled above the study area to determine lithologic and strength characteristics of the overburden strata using the rock samples collected. Electronic recorders were installed on all monitoring wells to continuously monitor ground water levels in coordination with mining of the longwall panels. A combined finite element model of the deformation of overlying strata, and it's influence on ground water flow was used to define the change in local and regional water budgets. The predicted effects of the postmining ground water system determined by the model correlated well with field data collected from the fieldsite. Without an infiltration rate added to the model, a static decrease of 3.0 m (10 ft) in water level would occur due to mining of both longwall panels and if an infiltration rate was inputted in the model, no predicted long-term effects would occur to the ground water system.

[1]Mining engineer, Pittsburgh Research Center, U.S. Bureau of Mines, Pittsburgh, PA.
[2]Research assistant, Pennsylvania State University, Department of Mineral Engineering, University Park, PA.
[3] Associate professor, Pennsylvania State University.

INTRODUCTION

Longwall mining is a method used to extract large blocks of coal. During extraction of the block, the immediate overburden is allowed to collapse, filling the void created by the excavation. Mining-induced strains and displacements are transferred throughout the overburden rock mass due to this collapse and the resultant stress redistribution creates changes to the ground surface and any water-bearing zones located above the mining area. Previous studies have been conducted to delineate the effects of longwall mining on the local ground water system (*1-9*).[4] Few of these studies, however, have used actual field data, in conjunction with numerical modeling, to determine and predict mining effects on the ground water regime. The U.S. Bureau of Mines (USBM) is studying the overburden rock mass and its response to high-extraction mining operations through a comprehensive program of field studies. The first part of the work involves the collection of mining, subsidence, overburden response, and hydrological data before, during, and subsequent to mining activity at numerous fieldsites. The second part of the program is examining methods of predicting the impact to local ground water supplies after mining activity occurs. One of these methods is through the application of numerical modeling.

MODEL APPROACH

An intensive surface, subsurface, and ground water monitoring program was conducted at a minesite in southeastern Ohio. Data collected from this site served as input information for a finite element (FE) model. The two-dimensional FE model incorporates the deformation of overlying strata and its influence on ground water flow through applying a simple relationship between mining-induced strains and changes in hydraulic conductivity. The strain field that develops around a longwall panel as a result of mining is material failure and self-weight. From this predicted strain field and from knowledge of the premining hydraulic properties of the overlying strata, the change in hydraulic conductivity that results from the strain field may be determined. With the modified conductivity field determined, the postmining hydrologic system may subsequently be defined through application of a ground water flow model. Again, this ground water flow model utilizes the FE method to determine the postmining hydrologic system where the position of the piezometric surface indicates changes in well or aquifer yields. This methodology is used to evaluate the influence of mining on the local ground water regime in this study.

THEORETICAL ANALYSIS OF MODELING APPROACH

The following assumptions are made when operating the model: (1) the rock matrix is functionally impermeable in comparison with fractures; (2) fluid flow in fractures is defined on the basis of the parallel plate model; (3) changes in fracture conductivity result from changes in normal strains only; (4) strains are partitioned between fractures and matrix as defined by a modulus reduction factor, R_m; and (5) fracture spacing, S, does not change after mining activity (*10-11*).

CORRELATION OF INDUCED STRAIN AND HYDRAULIC CONDUCTIVITY

The equivalent porous medium conductivity, K_o, of a rock mass containing a parallel set of fractures can be defined as:

$$K_o = \frac{g}{12 v_k} \frac{b^3}{S} \qquad (1)$$

where g is gravitational acceleration, v_k is kinematic viscosity, b is the fracture aperture, and S is spacing. R_m, the modulus reduction factor may be defined as:

$$R_m = \frac{E}{E_r} \qquad (2)$$

where E is the deformation modulus of the rock mass and E_r is the deformation modulus of a rock specimen. The modulus reduction factor, R_m, enables the closure across a fracture, Δu_j, to be determined from the difference between the strains in the rock mass and rock specimen as shown below:

$$\Delta u_j = [b + S (1 - R_m)] \Delta \epsilon \qquad (3)$$

where $\Delta \epsilon$ is the strain in the direction perpendicular to the fracture plane. $\Delta \epsilon$ is positive in extension and negative in compression.

---

[4]Italic numbers in parentheses refer to items in the list of references at the end of this report.

Using the applied strain, $\Delta\epsilon$, from above, the revised conductivity of equation 1 may be defined as:

$$\mathbf{K} = \mathbf{R_c K_o} \tag{4}$$

where

$$\mathbf{R_c} = \left[1 + \frac{b + S(1 - R_m)b^3}{b} \right]\Delta\epsilon \tag{5}$$

Directional conductivities, evaluated from initial conductivities, K_{ox} and K_{oy} (conductivities in the x- and y- directions, respectively) may then be determined from equation 4. With two sets of orthogonal fractures oriented in the x and y directions, the revised directional conductivities may be defined for a two-dimensional system as:

$$\mathbf{K_x} = \mathbf{K_{xo}} \left[1 + \frac{b + S(1 - R_m)}{b}\Delta\epsilon_y \right]^3 \tag{6}$$

and

$$\mathbf{K_y} = \mathbf{K_{yo}} \left[1 + \frac{b + S(1 - R_m)}{b}\Delta\epsilon_x \right]^3 \tag{7}$$

where K_x and K_y are postmining conductivities in the x-direction and the y-direction, K_{xo} and K_{yo} are the premining conductivities in the x-direction and the y-direction and $\Delta\epsilon_x$ and $\Delta\epsilon_y$ are the induced strains in the x and y directions, respectively. When $R_m = 1$, the mass modulus and intact material modulus are identical and the strain is uniformly distributed between fractures and matrix. This results in the smallest possible change in conductivity. When $R_m = 0$, the extensional strain is applied entirely to the fracture system and precipitates the largest possible change in conductivity. These values bound the possible ranges in the behavior of the system in a natural and mechanistically defensible manner. This representation of conductivities is extremely useful, since R_m may be readily evaluated from rock mass classification systems defining structural behavior as a function of readily observable factors of rock structure (12). This avoids the difficulty of defining conductivity enhancement in terms of the component moduli of fractures and matrix, parameters that are unlikely to be available in practice. The mining-induced conductivity changes can then be evaluated through equations 6 and 7, provided the mining-induced strain field is determined.

DETERMINATION OF STRAIN FIELD

The subsidence field that develops around a longwall panel may be determined directly from the FE model. The FE model applies gravitational load, removes material excavated from the panel and allows the overburden material to fail and deform according to the mining-induced strains. The resulting subsidence field may use R_m to calibrate against field data for a particular site. The insensitivity of the resulting subsidence profile to the material properties of deformation modulus and rock strength parameters, originates from the overriding influence of geometric controls on deformation (13-14). Following mining, the panel span is sufficiently large that closure between panel floor and roof is unavoidable. Consequently, the resulting strain field, ϵ_x and ϵ_y is defined purely as a function of geometry, as:

$$\epsilon_x, \epsilon_y = \mathbf{f}\left[\frac{w}{t}, \frac{w}{h} \right] \tag{8}$$

where w, represents the width of the panel, t is the thickness of the coalbed and h symbolizes the thickness of the overburden.

The assumption necessary in this evaluation is that strains are uniformly distributed at the scale of a single element. These assumptions seem reasonable where strains are moderate, but may be questionable where significant strain localization occurs.

DETERMINATION OF POSTMINING GROUND WATER REGIME

With the modified conductivity distribution determined from an evaluation of the strain field, and equations (6) and (7), the influence on the postmining ground water regime may be evaluated. The FE model may determine the influence of a continuously distributed conductivity field (evaluated from the calculated strain distribution) on the ground water budget and water table where boundary conditions are applied to the local system, to represent ground water and surface recharge. Therefore, the change in elevation of the phreatic surface may be determined for the postmining regime. This enables the influence of mining on well yields, aquifer yields, and flow patterns to be identified.

INPUT PARAMETERS USED FOR MODELING APPROACH

The primary parameters used as input to the model and the measurements obtained from the field are (1) the initial hydraulic conductivity distribution of the local lithology as determined through field measurements, (2) modulus of elasticity and Poisson Ratio values for the rock mass determined from field measurements, (3) the measured subsidence profile, (4) measured vertical displacements, (5) continuous fluid level fluctuations monitored at the site, and (6) flow rates entering the mine after excavation of the longwall panels, as recorded by the operator.

SITE DESCRIPTION AND GROUND WATER MONITORING PROGRAM

Site Description

The study site is located in southeastern Ohio (Vinton County). The study area overlies a portion of two contiguous longwall panels (Panels 1 and 2) measuring approximately 300 m (900 ft) wide and 2,950 m (9,000 ft) long (figure 1). The panels were separated by a five entry, four pillar system approximately 120 m (350 ft) wide. The mined coalbed, had an average thickness of 140 cm (55 in) within the study area. However, the extraction thickness varied between 173 and 183 cm (68 and 72 in). Overburden thickness was small and ranged from 65 to 85 m (214 to 280 ft). Overall, the strata were fairly level with a regional dip of about 1° towards the southeast. There were no major geologic structures and the topography consisted mainly of rolling hills with a maximum relief of approximately 49 m (160 ft).

Figure 1
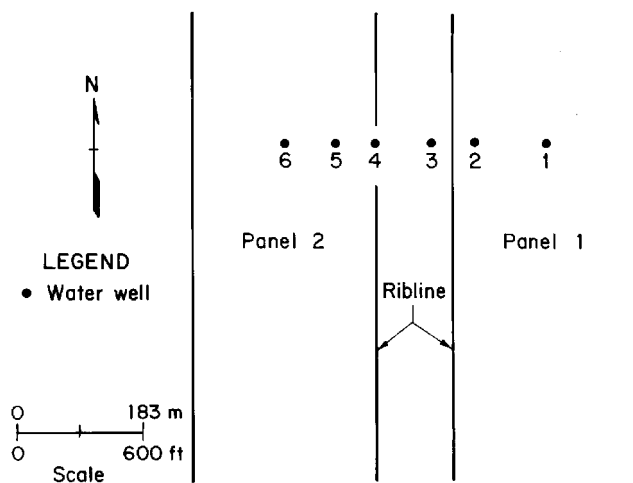
Sketch of study area.

Ground Water Monitoring Program

A total of seven 22-cm (8-5/8 in) diameter monitor wells were drilled for the study. Perforated Schedule 80 (15-cm diameter) (6-in) polyvinylchloride (PVC) casing was installed to the total depth in each well to ensure an open wellbore for the life of the study. The wells were strategically placed above both longwall panels as shown in figure 2. The wells were located along a line perpendicular to the trend of the longwall panels. This alignment permitted observations of effects during the mining of both longwall panels. Wells 1 and 6 were located at the center of panels 1 and 2, respectively. Wells 2 and 5 were located at quarter-panel width. Well 3 was located above the gate roads between the two panels and Well 4 was located above the edge of panel 2. Well 7, a control well, was located 427 m (1,400 ft) away from any mining activity.

Data were collected from all wells before, during, and after mining of both longwall panels. Various hydrologic parameters were determined and included specific capacity, transmissivity, hydraulic conductivity, and water level fluctuations. Initial data collection began 3 months prior to the undermining of Well 1 to establish baseline conditions. Drawdown and recovery pumping tests were performed on all wells before and after undermining to determine hydraulic conductivity parameters of the local, shallow geologic units.

Electronic recorders were also installed on all wells to continuously monitor water level fluctuations. The electronic data logger was programmed to record fluid positions every 4 h.

GEOLOGY

The geological setting of the study area is typical of that found in southeastern Ohio. The regional dip in this part of the State is to the southeast with the strata striking in a northeast-southwest direction. The average rate of dip is 6 m/km (30 ft/mi). Irregularities to this rate can be experienced by localized thinning or thickening of individual rock units (6). The rock is predominantly interbedded sandstones, shales, thin coal seams, and claystones. The individual units are thin (less than 3 m (10 ft) thick) with one sandstone unit (Vanport Limestone) having an average thickness of 14 m (45 ft) and lying 43 m (140 ft) above the Clarion 4A Coalbed. To characterize overburden lithology prior to drilling the monitoring wells, six 5.1 cm (2 in) coreholes were drilled at the study area to the Clarion 4A Coalbed. Generally, the overburden consisted of about 30% sandstone, 30% shale, 30% claystone, and 10% coal. A generalized cross-section of the study area with the monitor well locations is shown in figure 2.

Figure 2
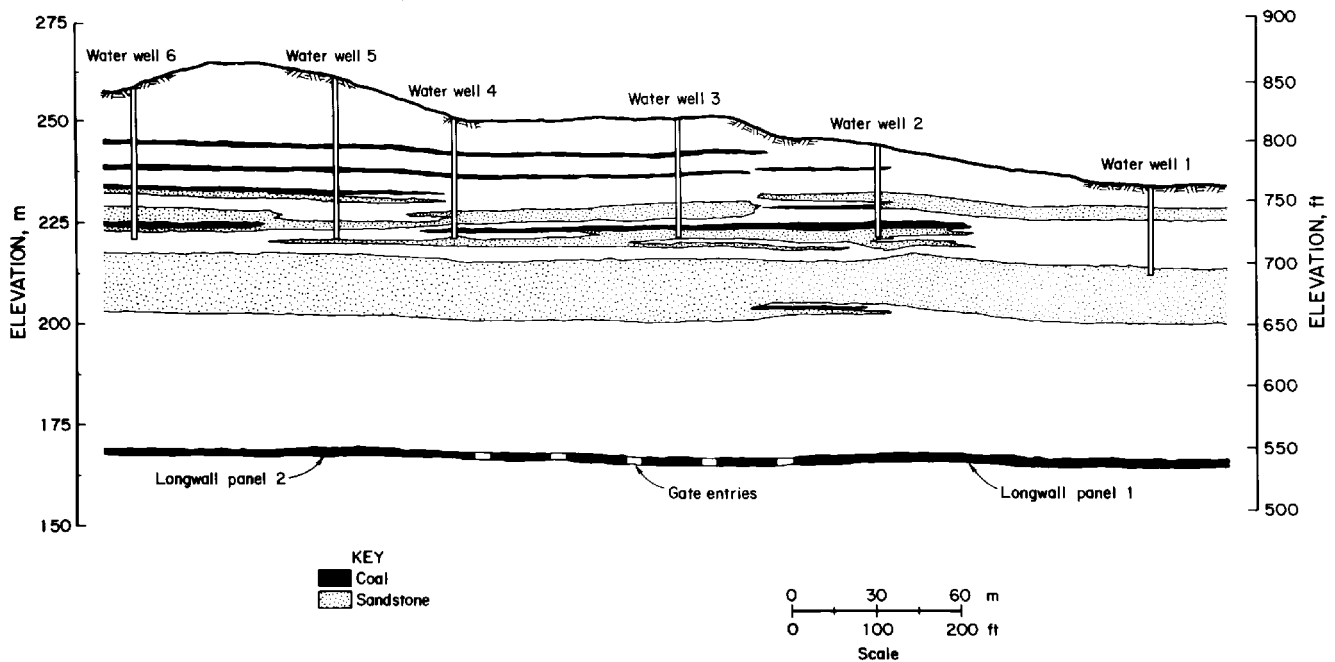
Generalized cross section of study area and Water Well locations.

MODULUS OF ELASTICITY AND POISSON RATIO VALUES

The coreholes were drilled above the study area to characterize the local lithology of the overburden and to provide samples for determining geotechnical properties. For input to the model, tests for determining compressive strength, Modulus of Elasticity, and Poisson Ratio were conducted on the rock cores collected. Results of tests performed on the core samples showed that the unconfined compressive strength of the major sandstone units are between 37 and 41 MPa (5,300 to 6,000 psi). Modulus of Elasticity and Poisson Ratio for these units are between 17,700 to 19,450 MPa (2.57 to 2.82 × 10⁶ psi) and 0.30 to 0.32, respectively. A limestone unit, averaging 2.1 m (7 ft) in thickness, is situated about 1 m (3 ft) above the mined coalbed. Testing of core samples show that the unconfined compressive strength of this unit is 172 MPa (25,000 psi), with a Modulus of Elasticity of 72,400 MPa (10.5 × 10⁶ psi), and a Poisson Ratio of 0.28.

OVERBURDEN DEFORMATION MONITORING PROGRAM

To observe overburden displacement, six 219.1 mm (8-5/8 in) boreholes were drilled along a profile line extending across the two longwall panels. Boreholes 1 and 6 were located in the center of each panel, where the maximum amount of subsidence was expected to occur. Boreholes 2 and 5 were

located 30 m (91 ft) from the ribline inside each panel. Borehole 4 was situated 3 m (10 ft) from the ribline (inside the panel) in the expected zone of maximum horizontal tension. Borehole 3 was located in a pillar in the gate entries between the panels to observe the lateral extent of overburden deformation.

Each borehole was outfitted with an eight-anchor MPBX. Two of the eight anchors in borehole 3 were installed inside a coal pillar to monitor yielding of the pillar. The anchors are numbered 1 to 8, with anchor 1 being the closest to the surface and anchor 8 being the deepest. Figure 3 displays MPBX and anchor locations with respect to the longwall panels.

SUBSIDENCE MONITORING PROGRAM

To obtain the field subsidence profile, survey monuments were installed on the ground surface and were surveyed regularly to identify the dynamic characteristics of subsidence, the final subsidence profile, and to provide surface reference data for the MPBX units. The monuments were constructed of 1.3 m (4 ft) rebar and were installed to the ground surface. The array of monuments consisted of a baseline (along the centerline) over each panel and a profile line trending perpendicular between the two baselines. The monuments were spaced 15 m (45 ft) apart along the baseline. The profile line was 375 m (1,136 ft) long with monuments spaced 7.5 m (23 ft) apart.
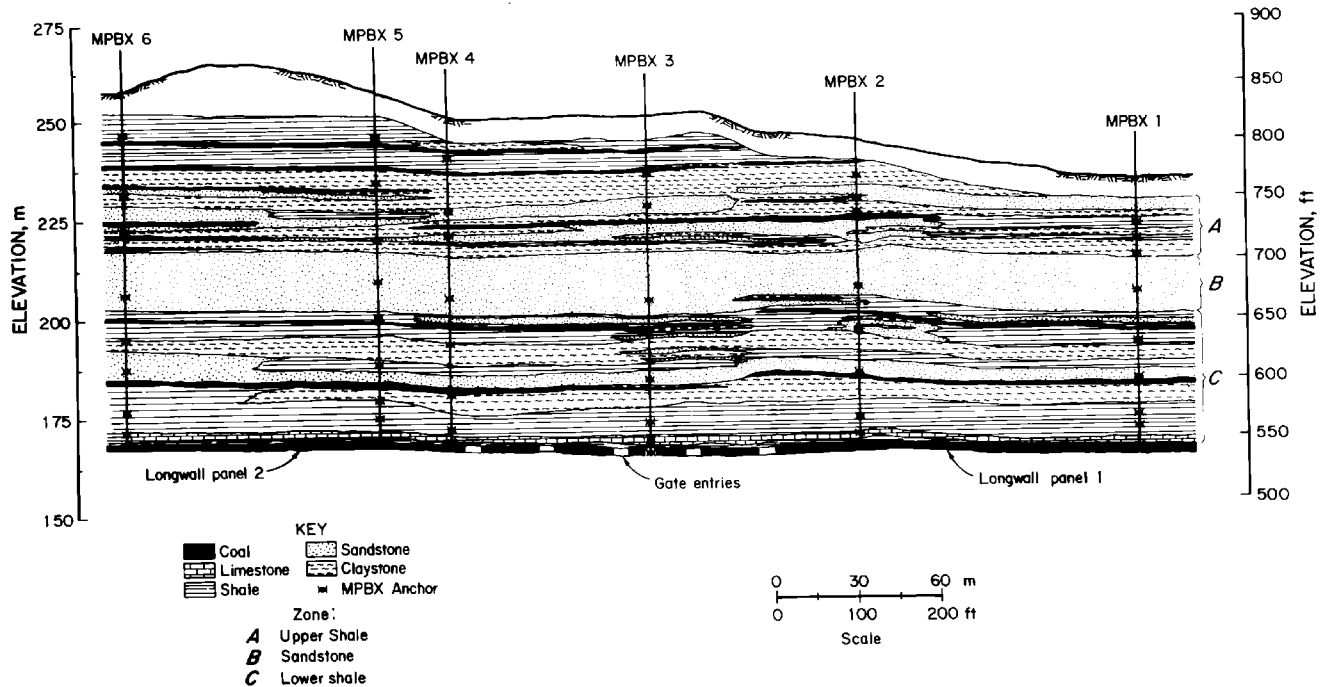
Generalized cross section of study area and MPBX locations.

MODEL ANALYSIS

FINITE-ELEMENT MESH ASSEMBLAGE

The finite-element mesh construction was assembled utilizing figure 3. The effects of topography, geometry, and lithology were incorporated in the mesh. The mesh utilizes uniform spacing and was constructed of 2,066 nodes and 1,928 elements. The mesh assumes differing materials (overburden material and coal layer) for the determination of strain and displacement characteristics, and three materials (upper shale layer, sandstone layer, and lower shale layer) for determination of the postmining flow characteristics within the system. The boundary conditions of the model for determining displacement and strain characteristics assume no horizontal movement on either side of the mesh and no vertical movement on the base. Boundary conditions associated with monitoring postmining ground water effects assume no flow on the bottom of the mesh and constant head conditions on the lateral sides of the mesh. The FE model is two-dimensional and determines the strain field with two displacement degrees of freedom applied to each node, and subsequently evaluates the revised flow system using a single degree of freedom. The analyses are

coupled through the dependence of hydraulic conductivity on the induced strain field, as defined in equations 6 and 7.

SUBSIDENCE PROFILE

The subsidence profile (figure 4), generated by the model, was determined with the input parameters as shown in table 1.

The values of the modulus of elasticity for the overburden were based on lab results obtained from core samples collected from the fieldsite. To obtain the model inputs, an average of all field samples was calculated (31,000 MPa) (4.4×10^6 psi) and ratios of 1/20 for the overburden material and 1/200 for the coal material were applied to the average lab result. Prior research has shown that decreasing E_{lab} values by several orders of magnitude, results in a better representation of actual field conditions and accounts for rock mass effects (*12*). Voight (*12*), has also noted that lab results within the range of 6,900 to 690,000 MPa (1.0×10^6 and 1.0×10^8 psi) should be reduced by at least one order of magnitude. A value of 4.0 was inputted into the model for the postfailure ratio of $E_{in\ situ}/E_{failed}$. This ratio is simply a curve fitting parameter to match the

Figure 4
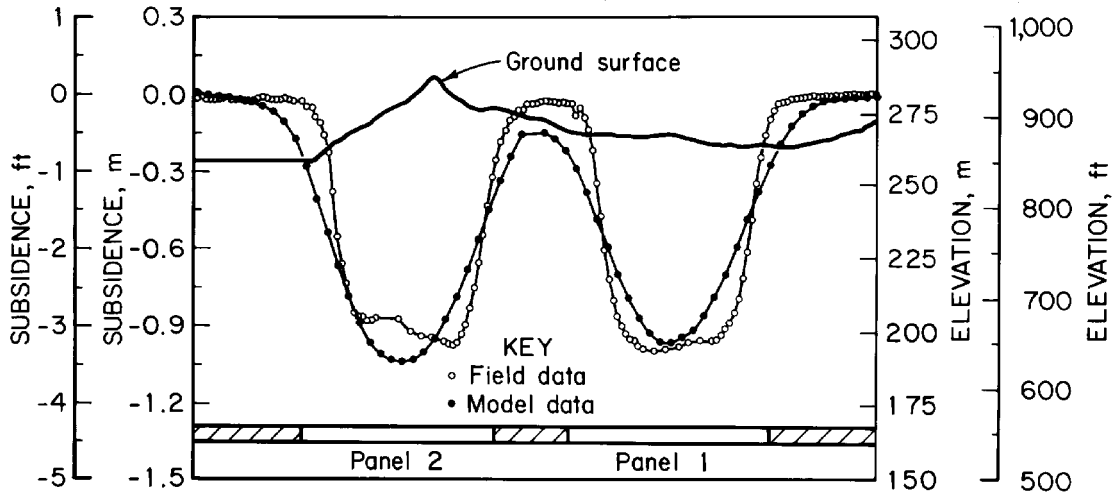
Comparison of field data and model subsidence profiles.

field-measured maximum subsidence magnitude with that derived from the model. In reality, the form of the subsidence profile predicted by the model is insensitive to the choice of elastic parameters. The excavation of coal is simulated using a bimodulus model. Initially, this material is assigned a very small modulus and a Poisson Ratio equal to zero, allowing the material to freely deform in the vertical direction. As the top and bottom of the panel contacts each other, the modulus of elasticity value is increased to prevent interpenetration.

Table 1.—Input parameters for generation of subsidence profile

Input parameter	Overburden material	Coal layer
E, MPa (psi)	1,550 (2.2×10^5)	1.56 (2.2×10^4)
n	0.30	0.30
D, kg/m^3(lb/ft^3)	2,400 (150)	390 (80)
$E_{in situ}/E_{failed}$	4.0	4.0
$n_{postfailure}$	0.450	0.450

D   Density.
E   Modulus of elasticity.
n   Poisson's ratio.

Figure 4 shows the subsidence profile determined by the model and the actual subsidence profile obtained from the collected field data. Although the two curves are not identical, the general trends of the curves are similar, with the maximum subsidence located above the two panels. This match is considered adequate for the subsequent hydrologic analyses.

COMPARISON OF VERTICAL DISPLACEMENTS DETERMINED BY MODEL AND FIELD DATA

Strain distributions are determined in the FE model by solving the boundary value problem with appropriate constitutive relations. The subsidence profile is the surface manifestation of this continuous redistribution of strain surrounding the mined panel. Strains and displacements generated within the mesh, as a result of mining, may also be determined and analyzed. A comparison of vertical displacements, within the overburden, as generated by the model and the displacements measured at the fieldsite are shown in tables 2-4.

The predicted vertical displacement data obtained from the model for MPBX's 1, 2, 3, and 6 correlate well with the field data collected at the site (tables 2-4). The field displacement data for MPBX 4 (table 3) showed minimal vertical displacement, whereas, the predicted vertical displacements for these boreholes showed slightly higher magnitudes of displacement (0.07 to 0.30 m) (0.22 to 0.99 ft). One contributing factor could be the difference between the predicted subsidence profile and the actual field data (figure 4). As displayed in the figure, the field data profile shows minimal amounts of subsidence occurring above the gate roads between the two panels. Whereas, the predicted subsidence profile shows a maximum of 0.15 m (0.5 ft) subsidence.

The anchors in MPBX 5 displayed larger magnitudes of vertical displacements compared with those predicted by the model. Again, this is mainly attributed to the differing shapes

of the subsidence profiles above the vicinity of the ribline over panel No. 2 (figure 4). The profile, developed from the model, shows less subsidence occurring above the ribline compared with the profile determined from the field data. As shown in the figure, the maximum subsidence (field data) for panel No. 2 occurs near the ribline, whereas, the model predicted maximum subsidence to occur above the center of the panel. This nonclassical form of the subsidence profile is attributed to site-specific geological conditions that are undefined and therefore not incorporated into the homogeneously distributed material parameters used in the finite element evaluation of displacements.

Table 2.—V_{field} versus V_{model} (vertical displacements) for MPBX Nos. 1 and 2

Borehole	Anchor	H		V_{field}		V_{model}	
		m	ft	m	ft	m	ft
1	1	54.56	179	1.14	3.73	1.00	3.28
	2	50.60	166	1.16	3.79	1.01	3.30
	3	47.00	154	1.17	3.85	1.01	3.30
	4	38.10	125	1.30	4.26	1.01	3.30
	5	25.91	85	1.50	4.90	1.01	3.30
	6	16.15	53	F	F	1.00	3.28
	7	8.53	28	F	F	1.00	3.25
	8	6.10	20	F	F	1.00	3.25
2	1	64.62	212	0.57	1.87	0.50	1.63
	2	57.91	190	0.57	1.87	0.50	1.63
	3	55.17	181	0.60	1.98	0.50	1.63
	4	38.71	127	0.70	2.27	0.51	1.68
	5	27.74	91	1.64	5.37	0.51	1.68
	6	18.59	61	F	F	0.52	1.71
	7	9.45	31	F	F	0.53	1.73
	8	5.18	17	F	F	0.53	1.74

F   Anchor failed.
H   Height above coalbed.

Table 3.—V_{field} versus V_{model} (vertical displacements) for MPBX Nos. 3 and 4

Borehole	Anchor	H		V_{field}		V_{model}	
		m	ft	m	ft	m	ft
3	1	70.10	230	0.00	0.00	0.09	0.29
	2	60.35	198	0.00	0.00	0.07	0.23
	3	36.90	121	0.00	0.00	0.07	0.22
	4	16.70	55	0.00	0.00	0.07	0.24
	5	7.01	23	0.00	0.00	0.07	0.24
	6	2.44	8	0.00	0.00	0.07	0.24
	7	0.91	3	0.00	0.00	0.07	0.24
	8	0.30	1	0.00	0.00	0.07	0.24
4	1	70.71	232	0.00	0.00	0.30	0.99
	2	58.52	192	0.00	0.00	0.27	0.88
	3	52.73	173	0.00	0.00	0.25	0.82
	4	36.88	121	0.00	0.00	0.21	0.70
	5	25.30	83	0.00	0.00	0.19	0.62
	6	13.41	44	0.00	0.00	0.16	0.52
	7	3.96	13	0.00	0.00	0.14	0.47
	8	1.83	6	0.00	0.00	0.12	0.41

H   Height above coalbed.

Table 4.—V_field versus V_model (vertical displacements) for MPBX Nos. 5 and 6

Borehole	Anchor	H		V_field		V_model	
		m	ft	m	ft	m	ft
5	1	83.21	273	1.21	3.97	0.56	1.85
	2	64.00	210	1.28	4.20	0.56	1.85
	3	50.30	165	1.43	4.70	0.56	1.84
	4	39.62	130	1.44	4.73	0.56	1.85
	5	31.10	102	1.53	5.01	0.56	1.85
	6	19.2	63	F	F	0.59	1.93
	7	10.36	34	F	F	0.60	1.96
	8	5.80	19	F	F	0.61	1.99
6	1	75.60	248	1.09	3.56	1.10	3.62
	2	62.79	206	F	F	1.11	3.63
	3	51.21	168	1.10	3.62	1.12	3.66
	4	38.10	125	F	F	1.12	3.66
	5	27.43	90	F	F	1.11	3.64
	6	19.50	64	1.14	3.73	1.11	3.61
	7	9.45	31	F	F	1.09	3.57
	8	3.96	13	F	F	1.08	3.53

F   Anchor failed.
H   Height above coalbed.

CORRELATION OF POSTMINING HYDROLOGIC REGIME
# WITH DATA COLLECTED FROM FIELDSITE

The postmining effects to the ground water system (figure 5), evaluated from the model, were determined though input of the parameters as shown in table 5.

Numerous drawdown and recovery pumping tests were performed on all the monitoring wells to determine hydraulic conductivity values. The hydraulic conductivity value of 7.01×10^{-8} m/s (2.3×10^{-7} ft/s), for the upper overburden material (shale), was determined by averaging the hydraulic conductivity values measured at the site. The estimated hydraulic conductivity value, 7.01×10^{-5} m/s (2.3×10^{-4} ft/s) for the sandstone material was used as input into the model. This value was three orders of magnitude greater than the measured conductivity value obtained for the upper overburden material. This value of hydraulic conductivity was used because it is believed that the sandstone unit provides a much higher permeability than that of a shale unit. The hydraulic conductivity for the lower overburden material (shale) was one order of magnitude less than that of the upper material 7.01×10^{-9} m/s (2.3×10^{-8} ft/s). Prior USBM research has shown that fractures within the overburden rock mass commonly decrease in aperture and number with increasing depth (13). Correspondingly, the rock mass at depth is assumed `tighter' and consequently less conductive.

The fracture spacing values used are assumed, since no information regarding fracture spacings were determined at the fieldsite. However, the selected values are consistent with those incorporated in other successful calibration studies (9-11). As mentioned earlier, the modulus reduction factor, R_m, reflects the partitioning of mining-induced strains between fractures and the porous matrix. In less stiff materials, the matrix accommodates proportionately more of the applied bulk strain than stiffer materials, where fracture closure dominates the mass response. Correspondingly, less competent materials, such as shales, return higher magnitudes of the modulus reduction factor. Without field measured magnitudes, appropriate magnitudes of the modulus reduction factor are selected, reflecting these anticipated characteristics of behavior.

Figure 5
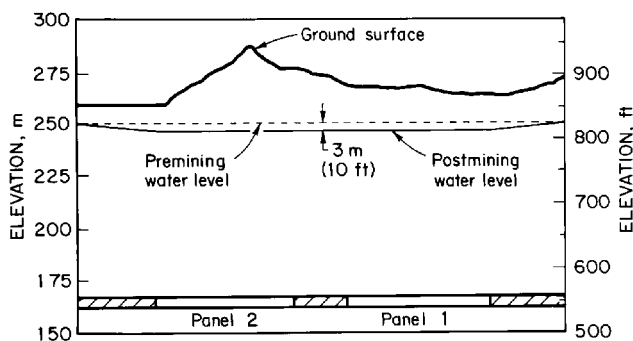
Postmining effects of ground water system - predicted by model. Flow rate - Q = 2,390 Lpm (630 gpm).

**Table 5.—Input parameters for determination of postmining ground water effects**

Input parameter	Overburden upper shale	Overburden sandstone	Overburden lower shale
K_x, horizontal conductivity	7.01×10^{-8} m/s	7.01×10^{-5} m/s	7.01×10^{-9} m/s
	$(2.3 \times 10^{-7}$ ft/s$)$	$(2.3 \times 10^{-4}$ ft/s$)$	$(2.3 \times 10^{-8}$ ft/s$)$
K_y, vertical conductivity	7.01×10^{-8} m/s	7.01×10^{-5} m/s	7.01×10^{-9} m/s
	$(2.3 \times 10^{-7}$ ft/s$)$	$(2.3 \times 10^{-4}$ ft/s$)$	$(2.3 \times 10^{-8}$ ft/s$)$
S, fracture spacing	0.31 m	0.91 m	0.10 m
	(1 ft)	(3 ft)	(0.30 ft)
R_m, modulus reduction factor ...	0.80	0.05	0.97
v, kinematic viscosity	1.0×10^{-6} m^2/s	1.0×10^{-6} m^2/s	1.0×10^{-6} m^2/s
	$(1.0 \times 10^{-5}$ ft^2/s$)$	$(1.0 \times 10^{-5}$ ft^2/s$)$	$(1.0 \times 10^{-5}$ ft^2/s$)$
g, acceleration of gravity	9.81 m/s^2	9.81 m/s^2	9.81 m/s^2
	(32.2 ft/s^2)	(32.2 ft/s^2)	(32.2 ft/s^2)
I, infiltration rate	0.23 m/yr	0.00	0.00
	(0.75 ft/yr)		

Flow rates entering the mine following the excavation of both panels were monitored by the mining company. Mine personnel estimated flow rates through the monitoring of a main sump located underground. Effects of surface area, lithology, and hydrogeology were incorporated into the analysis to determine flow rate estimates. This information provided a reasonable basis for the selection of several values for input into the model i.e., fracture spacing (S) and modulus reduction factor (R_m). The flow rate provided by the mining company was approximately 2,390 Lpm (630 gpm). Values of R_m, determined through matching the flow rate, were 0.80 for material 1, 0.05 for material 2, and 0.97 for material 3. Choice of these parameters was clearly nonunique, but was predicted on the anticipated response of the lithologic units to straining and fracturing. The preexisting fractures in the upper shale and the lower shale units have less effects on the postmining conductivities than those in the sandstone layer unit. Actually, the shale material may be treated as a porous medium which is not sensitive to deformation. The difference between the two values is due to the effect of depth. The value of R_m is chosen as 0.05 for the sandstone unit because a large part of the extensional strain is applied to the fracture system and precipitates the largest possible change in conductivity.

The coarse finite element mesh, used to evaluate the subsidence profile and overburden displacements, was applied to determine the influence of mining-induced permeability changes on the ground water system. The predicted effects on the postmining ground water system determined by the model correlated well with the field data collected at the site as shown in figures 6-11. Figures 6-11 show water level fluctuations measured for Wells 1-6, respectively. In addition, curves were added to the figures which show progression of the longwall face as a function of the overburden thickness. These values are expressed as the ratio of face position (FP) to overburden thickness (OB). For example, consider a longwall face that is moving towards a well, but is 183 m (600 ft) away and the overburden at the site of the well is 61 m (200 ft). The FP/OB ratio is -3. The negative value of FP/OB ratio indicates a premining position of the longwall face; zero indicates when the respective longwall face passed beneath the line of wells; and a positive value indicates postmining positions of the longwall face past the line of wells. If at another site a longwall face was approaching a well, but was 366 m (1,200 ft) away and the thickness of the overburden at the site of the well was 122 m (400 ft), the FP/OB ratio is still -3. This curve allows one to compare well response at two different sites (conceivably in the same study area) without having to make complicated adjustments for differing overburden thicknesses. Under the applied boundary conditions, the model determined that a static decrease of 3.0 m (10 ft) in water level would occur due to the mining of both longwall panels. This decrease would occur without an infiltration rate inputted in the
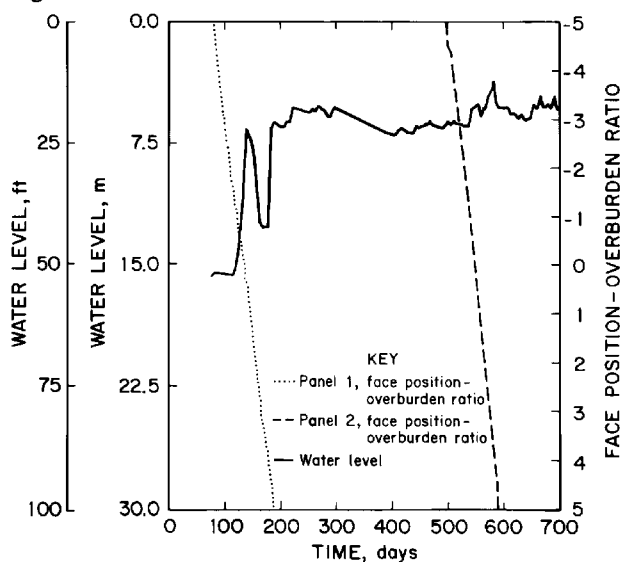
Figure 6

KEY
.... Panel 1, face position - overburden ratio
– – Panel 2, face position - overburden ratio
—— Water level
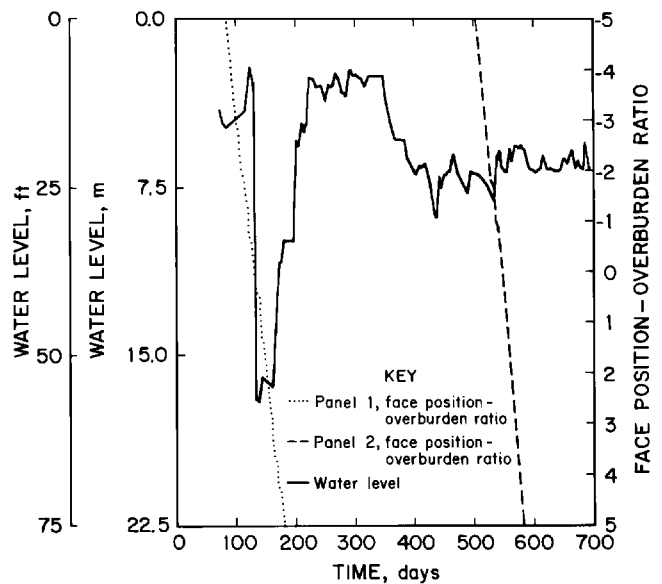
Comparison of water level change and face position to overburden ratio for Well 1.
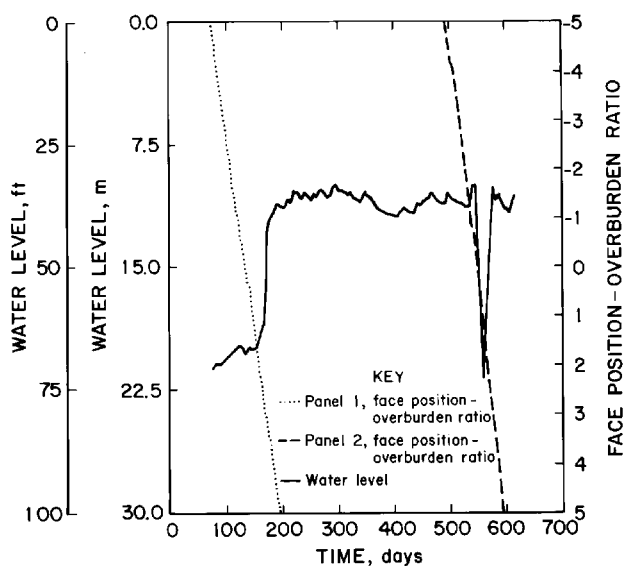
Figure 7
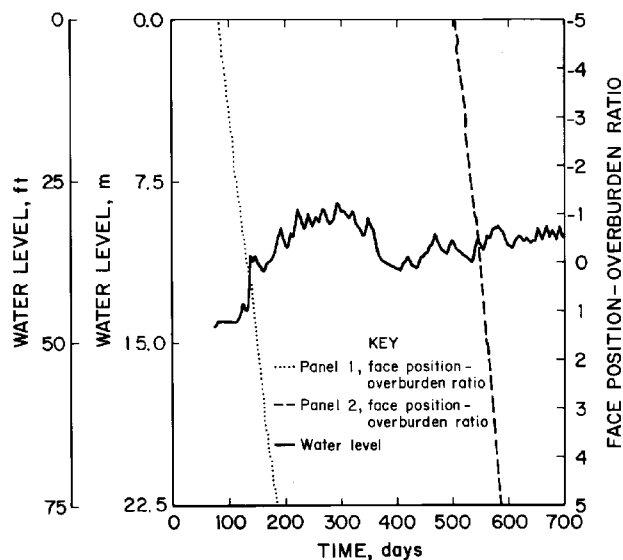
Comparison of water level change and face position to over-
burden ratio for Well 2.

Figure 8

Comparison of water level change and face position to over-
burden ratio for Well 3.

Figure 9

Comparison of water level change and face position to over-
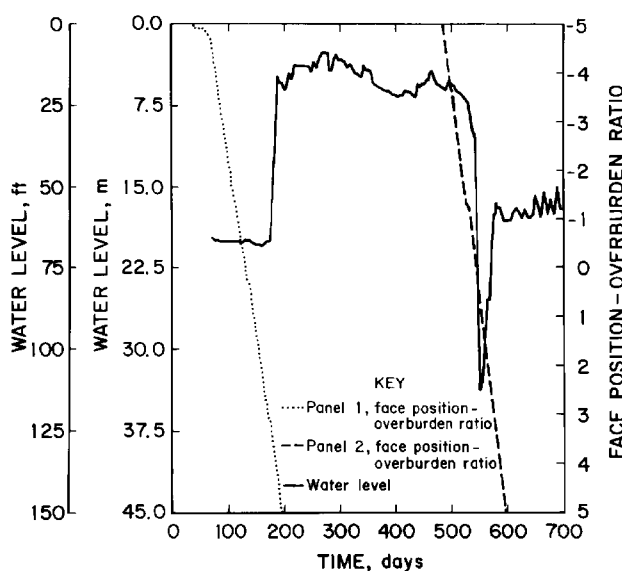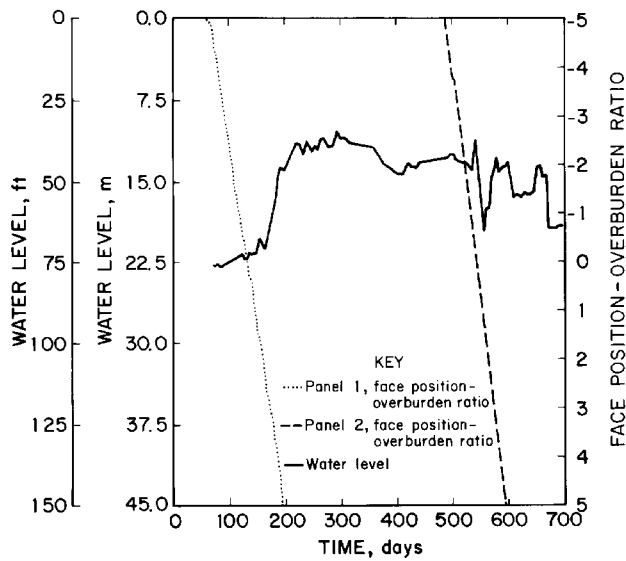burden ratio for Well 4.

Figure 10

Comparison of water level change and face position to over-
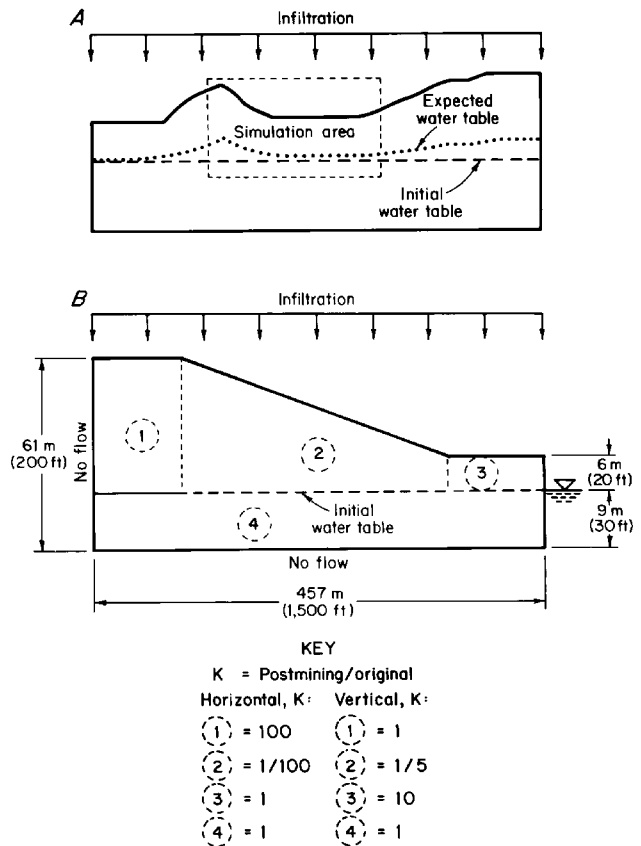burden ratio for Well 5.

Figure 11

Comparison of water level change and face position to over-
burden ratio for Well 6.

Figure 12

Model for topographic influence of infiltration on well ele-
vations. A, Conceptual; B, numerical.

model. If an infiltration rate of 0.23 m/yr (0.75 ft/yr) is used, the regional model predicts that essentially no effects to the static phreatic surface would result. This infiltration rate is 25% of the total precipitation occurring at the site and correlates well with known infiltration rates of previous studies (*14*). Precipitation records provided by the mining company showed an average precipitation of 0.91 m (3.0 ft) which occurred at the site. Therefore, an infiltration rate of 0.23 m/yr (0.75 ft/yr) was used. Figure 5 shows the model prediction after excavation of both longwall panels.

In addition to applying the regional model, described above, local behavior around the shallow well field (figure 12*A*) was also represented by a more refined model to accommodate more subtle water budget changes as a result of mining. The changes in hydraulic conductivities predicted from the initial calculations were applied to the zonation as defined in figure 12*B*. These zones represent average changes in hydraulic conductivities evaluated from the subsidence modeling. The refined mesh is capable of accurately representing local changes in the location of the phreatic surface. This mesh represents the region between the centerlines of both panels containing Well 5 and 6 within Zone I, Wells 2 to 4 within Zone II, and Well 1 within Zone III. No flow boundary conditions were specified along the base and on the left side (the centerline of panel No. 2) and constant head conditions were applied on the remaining vertical side (about 76.2 m (250 ft) away from the centerline of panel No. 1). The mesh, utilized uniform spacing, and was constructed of 326 nodes and 295

elements. Two different situations were simulated through use of the refined mesh. First, the same infiltration rate and premining ground water conditions were inputted, where the small-scale influences of topographically induced flow were accommodated. Second, the postmining hydraulic conductivity magnitudes of table 5 were incorporated to determine the anticipated postmining ground water levels. The magnitude of hydraulic conductivities was evaluated directly from the spatial distribution of strains, using equations 6 and 7. Average magnitudes of horizontal and vertical conductivities were then utilized in the refined model of figure 12. The changes in hydraulic conductivities are documented in table 6.

The resulting postmining modification in the location of the phreatic surface is illustrated in figure 13. The subtle changes result from applying the same infiltration rate as used in the previous model run, however, the greater element density of this revised model highlights the influence of even minor topography and moderate changes in near surface hydraulic conductivities on the ground water system. The

Figure 13

KEY
- - - Premining water table
——— Postmining water table (model)

0   30   60 m
0   100   200 ft
Scale
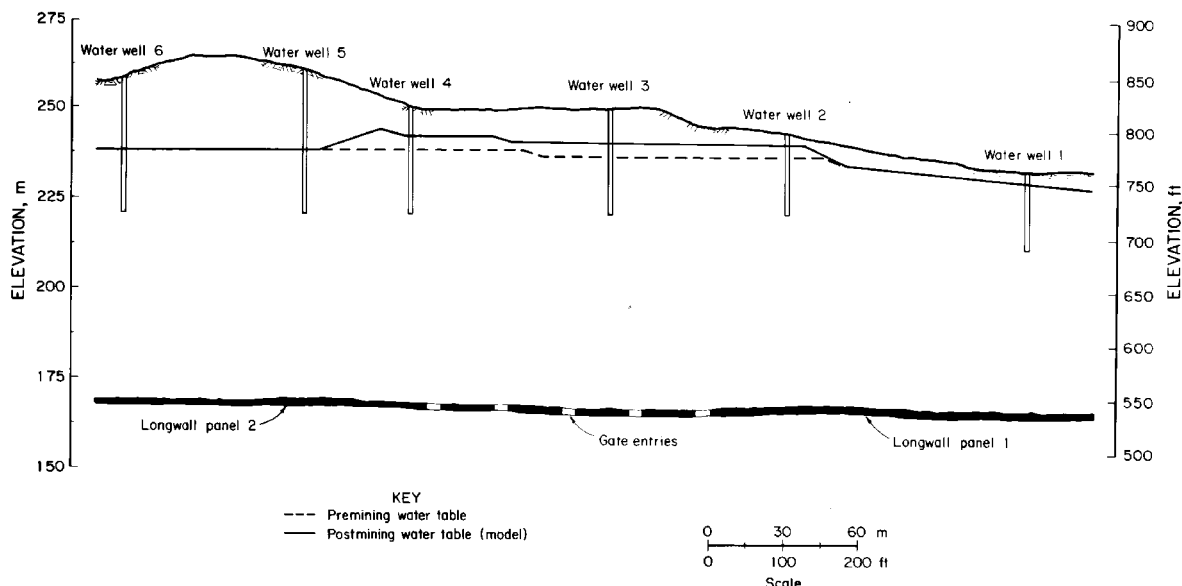
Postmining effects on ground water system using smaller-scale mesh around well area.

water system. The mining-induced development of hydraulic conductivities is such that water levels in the region of Wells 5 and 6 remain the same, water levels in the region of Wells 3 and 4 rise, and water levels in the region of Wells 1 and 2 fall, relative to premining water levels. When the long-term recorded levels in these six wells are corrected relative to the control well (a well located approximately 425 m (1,400 ft) away from mining activity), this distribution of behavior, and of this magnitude is exactly as observed from the field measurements performed at the site (*6*) and as shown in figures 6-11.

Table 6.—Relative changes in hydraulic conductivity ($K_{postmining}/K_{original}$) as applied to small-scale mesh

Zone	K_h	K_v
1	100	1
2	1/100	1/5
3	1	10
4	1	1

K_h Horizontal conductivity.
K_v Vertical conductivity.

SUMMARY

1. The subsidence profile, as determined from the model, compares favorably with maximum subsidence measured at the fieldsite.

2. The field data showed that minimal subsidence occurred above the gate roads between the two panels, while the predicted subsidence profile showed a maximum of 0.15 m (0.5 ft) subsidence at this location.

3. The predicted vertical displacement data obtained from the model for MPBX's 1, 2, 3, and 6 correlated well with the field data.

4. The field displacement data for MPBX 4 displayed minimal displacements, whereas, the predicted displacements

for these boreholes showed slightly higher displacement. Also, MPBX 5 showed similar vertical displacements compared with that predicted by the model.

5. The predicted effects of the postmining ground water system determined by the model correlated well with the field data collected at the site. Without infiltration added, the model determined that a static decrease of 3.0 m (10 ft) in water level would occur at the site due to the mining of both longwall panels 1 and 2. If an infiltration rate was input to the model, no predicted effects for the long term would occur to the ground water regime which correlates well with field observations.

6. Where a fine mesh is used to define local changes in water budget within the well field area, the model is capable of replicating relatively subtle changes in long-term water levels.

Minor local changes in the phreatic surface are consistent with the rolling topography of the site and the effects of mining-induced changes in hydraulic conductivity.

CONCLUSIONS

For this study, the numerical modeling results correlate favorably with the field data collected at the site. The surface subsidence information from the field, provided an excellent foundation for the modeling routine. If this information is not available, one should obtain and examine available subsidence prediction models to determine the profile information for the site. The assumptions made during the course of operating the model were based on knowledge of the subject area, experience with the model and insight gained from field tests. Again, if the field information is not available, the model routine requires some additional assumptions. Although a favorable correlation exists between the mining effects predicted and the field data collected, the authors feel that additional comparative studies at research sites with varying geology, longwall panel characteristics (thickness, width, etc.), hydrogeology, etc. should be performed to further substantiate the capabilities of the model.

REFERENCES

1. Johnson, K. L. Influence of Topography on the Effects of Longwall Mining on Shallow Aquifers in the Appalachian Coalfield. Paper in Proceedings of the 3rd Workshop on Surface Subsidence Due to Underground Mining (Morgantown, WV, June 1-4, 1992). WVU, 1992, pp. 197-203.

2. Booth, C. J. Hydrogeologic Impacts of Underground (Longwall) Mining in the Illinois Basin. Paper in Proceedings of the 3rd Workshop on Surface Subsidence Due to Underground Mining (Morgantown, WV, June 1-4, 1992). WVU, 1992, pp. 222-227.

3. Leavitt, B. R., and J. F. Gibbens. Effects of Longwall Coal Mining on Rural Water Supplies and Stress Relief Fracture Flow Systems. Paper in Proceedings of the 3rd Workshop on Surface Subsidence Due to Underground Mining (Morgantown, WV, June 1-4, 1992). WVU, 1992, pp. 228-235.

4. Tieman, G. E., and H. W. Rauch. Study of Dewatering Effects at a Longwall Mine in Northern West Virginia. Paper in Proceedings of the 3rd Workshop on Surface Subsidence Due to Underground Mining (Morgantown, WV, June 1-4, 1992). WVU, 1992, pp. 214-221.

5. Matetic, R. J., and M. A. Trevits. Case Study of Longwall Mining Effects on Water Wells. Paper in Proceedings of the SME Annual Meeting (Salt Lake City, UT, Feb. 26-Mar. 1, 1990). SME preprint 90-141, 1990, 7 pp.

6. Matetic, R. J., Trevits, M. A., and T. Swinehart. A Case Study of Longwall Mining and Near-Surface Hydrological Response. Paper in Proceedings of the 1991 American Mining Congress Coal Convention (Pittsburgh, PA, June 2-5, 1991). AMC, 1991, pp. 445-472.

7. Matetic, R. J., and M. A. Trevits. Longwall Mining and its Effect on Ground Water Quantity and Quality at a Mine Site in the Northern Appalachian Coalfield. Paper in Proceedings of the FOCUS Conference on Eastern Regional Ground Water Issues (Newton, MA, Oct. 13-15, 1992). Water Well J. Publ. Co., 1992, pp. 573-587.

8. Trevits, M. A., and R. J. Matetic. A Study of the Relationship Between Saturated Zone Response and Longwall Mining-Induced Ground Strain. Paper in Proceedings of the 5th Outdoor Action Conference on Aquifer Restoration, Ground Water Monitoring and Geophysical Methods (Las Vegas, NV, May 13-16, 1991). Water Well J. Publ. Co., 1991, pp. 1101-1109.

9. Elsworth, D., J. Liu, and Z. Ouyang. Some Approaches to Determine the Potential Influence of Longwall Mining on Ground Water Resources. Paper in Proceedings of the International Land Reclamation and Mine Drainage Conference and Third International Conference on the Abatement of Acidic Drainage (Pittsburgh, PA, Apr. 24-29, 1994). V. 4, NTIS, 1994, pp. 172-179.

10. Liu, J. Topographic Influence of Longwall Mining on Water Supplies. M.S. Thesis, The Pennsylvania State Univ., University Park, PA, 1994, 73 pp.

11. Ouyang, Z., and D. Elsworth. Evaluation of Groundwater Flow into Mined Panels. Int. J. Rock Mech., Miner. Sci. and Geomech. V. 30, No. 2, 1993, pp 71-79.

12. Voight, B., and W., Pariseau. State of Predictive Art in Subsidence Engineering. J. Soil Mech. and Foundations Div., v. 96, No. SM 2, 1970, pp. 721-750.

13. Walker, J. S., J. B. Green, and M. A. Trevits. A Case Study of Water Level Fluctuations Over a Series of Longwall Panels in the Northern Appalachian Coal Region. Paper in Proceedings of the 2nd Workshop on Surface Subsidence Due to Underground Mining (Morgantown, WV, June 9-11, 1986). WVU, 1986, pp. 264-269.

14. Stoner, J. D. Probable Hydrologic Effects of Subsurface Mining. Ground Water Monitoring Rev., winter 1983, pp. 128-138.